Structural Dynamics of HIV-1 Rev and Its Complexes with RRE and 5S RNA

Wai-Chung Lam,[‡] Jan M. Seifert,[§] Franz Amberger,[§] Christine Graf,[§] Manfred Auer,*[,§] and David P. Millar*[,‡]

Department of Molecular Biology, MB-19, The Scripps Research Institute, 10550 North Torrey Pines Road, La Jolla, California 92037, and Novartis Research Institute, Brunnerstrasse 59, A-1235 Vienna, Austria

Received August 4, 1997; Revised Manuscript Received December 3, 1997

ABSTRACT: The Rev protein of the human immunodeficiency virus type 1 (HIV-1) has been studied by time-resolved fluorescence spectroscopy. The single tryptophan residue of Rev, Trp45, located within the arginine-rich RNA-binding domain of the protein, was utilized as an intrinsic spectroscopic probe. In addition, five peptides spanning different lengths of the arginine-rich domain, each containing the tryptophan residue, and two C-terminal deletion mutants of Rev, Rev M9Δ14 and Rev M11Δ14, were examined. Rev M9Δ14 lacks residues 68−112 whereas Rev M11Δ14 is missing residues 92−112 of the C-terminus of Rev. The fluorescence decay of Trp45 in wild-type Rev was resolved into four discrete lifetime components, and decay-associated spectra (DAS) were obtained for each component. The fluorescence decays of all five peptides and Rev M9Δ14 were resolved into three lifetime components. The fluorescence decay of Rev M11Δ14 was resolved into four components similar to those found for wild-type Rev. These results indicate that the activation domain (residues 78−93), present in wild-type Rev and Rev M11Δ14, induced a unique tryptophan environment, characterized by a short-lived, blue-shifted emission, attributed to higher order assembly of Rev. In addition, fluorescence anisotropy decay data obtained for wild-type Rev and the two C-terminal deletion mutants also indicate that the activation domain mediates self-association of Rev. Based on the anisotropy decay results for wild-type Rev, the distribution of oligomers is independent of salt concentration. The average fluorescence lifetime of Trp45 was reduced upon complexation of Rev with a 40-mer fragment of the Rev response element containing the minimal element for Rev binding (F8-RRE), and the emission was blue-shifted. In addition, the local rotation of the tryptophan side chain was blocked in the protein−RRE complex. These results indicate that Trp45 directly interacts with the RRE. Rev is also shown to bind to 5S RNA, resulting in very similar changes in the time-resolved tryptophan fluorescence to those observed upon complexation of Rev with F8−RRE.

Rev is an important HIV-1[1] regulatory protein that is involved in the transport of unspliced and incompletely spliced viral mRNAs from the nucleus to the cytoplasm of the host cell (*1*−*4*). These mRNAs encode the structural proteins essential for viral replication (*5*, *6*), thus providing a therapeutic target in the treatment of HIV-1 infection. Rev binds to a part of the HIV-1 *env* gene called the Rev response element (RRE) (*3*, *7*−*9*). Stem−loop IIB of the RRE has been identified as a high-affinity binding site for Rev (*10*−*12*). A 17-amino acid arginine-rich region of Rev spanning amino acids 34−51 binds specifically to the RRE (*13*−*18*). The protein activation domain necessary to mediate the interaction of Rev with nuclear proteins involved in translocation of RNA to the cytoplasm is located between amino acids 78 and 93 (*19*−*21*). Rev is known to multimerize in the presence or absence of RNA (*13*, *22*). The addition of one more Rev monomer after the first monomer binds to the RRE adds to the stability of the Rev−RRE complex (*23*, *24*).

The elucidation of the three-dimensional structure of Rev by X-ray crystallographic or NMR spectroscopic methods has been impeded by the strong tendency of the protein to aggregate (*10*). To date, the only structural information on Rev has come from circular dichroism (CD) studies (*25*−*27*) and from NMR spectroscopic studies of a model peptide of the RNA-binding domain (*28*). These studies have shown that the arginine-rich RNA-binding domain adopts an α-helical secondary structure (*28*) and that the α-helical content of Rev remains unchanged upon binding to the RRE (*27*). An NMR-based structural model of a peptide spanning the arginine-rich region of Rev bound to a short target RNA sequence shows that the helical peptide is inserted into the major groove of the RNA near a purine-rich internal loop (*29*). However, higher order conformational changes of the RNA−protein complex due to full-length Rev and Rev−Rev multimerization cannot be studied in this minimal model system.

Fluorescence spectroscopy can provide a variety of information on protein structure and dynamics, including the local environment of tryptophan residues, the existence of protein conformers, and the rates of rotational diffusion and segmental motions. Moreover, fluorescence measurements

* Corresponding authors.
[‡] The Scripps Research Institute.
[§] Novartis Research Institute.

[1] Abbreviations: DTT, dithiothreitol; HIV-1, human immunodeficiency virus type 1; MES, morpholinoethanesulfonic acid; TBAF, tetrabutylammonium fluoride; THF, tetrahydrofuran; NaN_3, sodium azide; K_2SO_4, potassium sulfate; $(NH_4)_2SO_4$, ammonium sulfate.

S0006-2960(97)01909-0 CCC: $15.00
Published on Web 01/23/1998

can be carried out at low protein concentrations where aggregation does not dominate. Here, we present a time-resolved fluorescence study of Rev, utilizing the single tryptophan residue, Trp45, as an intrinsic spectroscopic probe. Trp45 is located within the arginine-rich RNA-binding domain of Rev and is appropriately positioned, therefore, to report on the conformation and dynamics of that domain and the interaction of the protein with its cognate RNA. The results of time-resolved fluorescence lifetime and anisotropy decay studies of wild-type Rev, two C-terminal deletion mutants, and a series of Rev peptides show that the tryptophan environment is influenced by multimerization of the protein mediated by the activation domain. Moreover, complexation of Rev with a 40-mer portion of the RRE, containing the minimal element for specific, high-affinity Rev binding, the F8 40-mer (*30*), causes a significant change in the time-resolved fluorescence properties of Trp45, showing that the tryptophan side chain directly interacts with the RRE. It is also shown that Rev can bind to 5S RNA and that the resulting changes in the time-resolved tryptophan emission are essentially identical with those caused by binding to the RRE, raising the possibility that these two RNA molecules access similar or identical export pathways from the nucleus to the cytoplasm.

MATERIALS AND METHODS

Expression and Purification of Rev, Rev M9Δ14, and Rev M11Δ14. Expression and purification of HIV-1 Rev and the C-terminal deletion mutants Rev M9Δ14 (residues 1−67) and Rev M11Δ14 (residues 1−91) have been described previously (*27*, *31*).

Peptide Synthesis. Rev peptides were synthesized using Fmoc methodology on an ABI synthesizer and purified to >95% purity by reversed-phase HPLC. The peptide sequences and purity were confirmed by amino acid analysis. The amino acid sequences of the Rev peptides used here are as follows: P1, RW; P2, RRRRWR; P3, NRRRRWRE; P4, RRNRRRRWRERQ; P5, TRQARRNRRRRWRERQRQ. These peptides correspond to different regions of the polypeptide chain of Rev surrounding the single tryptophan residue (Trp45 in Rev).

Chemical Synthesis of 40-mer F8−RRE. Sets of 5′-*O*-dimethoxytrityl-2′-*O*-*tert*-butyldimethylsilyl-protected ribonucleotide β-cyanoethyl-(*N*,*N*-diisopropyl)phosphoramidites and controlled pore glass supports (CPG, 500 Å pore size) with N^2-phenoxyacetylguanosine, N^6-phenoxyacetyladenosine, N^4-benzoylcytidine, and uridine were purchased from Glen Research (Sterling, VA). CPG supports with N^2-isobutyrylguanosine, N^6-benzoyladenosine, N^4-benzoylcytidine, and uridine were purchased from Milligen (Hamburg, Germany). Tetrazole (0.5 M in acetonitrile) was obtained from Applied Biosystems (Foster City, CA); anhydrous acetonitrile was purchased from Labscan (Dublin, Ireland). Other synthesis reagents were from Merck (Darmstadt, Germany; analytical grade reagents). Tetrahydrofuran was dried by passage through an aluminum oxide column, and *N*-methylimidazole was vacuum-distilled before use. 1.1 M tetrabutylammonium fluoride/THF was purchased from Aldrich (Vienna, Austria). Ribonuclease A, nuclease P1, and polynucleotide kinase were obtained from Boehringer Mannheim (Mannheim, Germany). Nucleotide triphosphates (100 μM solutions), alkaline phosphodiesterase, and ribonucleases V_1 and T_1 were purchased from Pharmacia LKB (Uppsala, Sweden). T7-RNA polymerase was obtained from Boehringer Mannheim, USB (Cleveland, OH), Promega (Madison, WI), and Dr. King Farrington, Repligen Corp., Cambridge, MA.

RNA oligonucleotides were synthesized using 0.1 M cyanoethylphosphoramidite monomers on an Applied Biosystems 394A synthesizer at the 1 μmol scale, adopting published procedures (*32*−*35*). Besides benzoyl protection for C, either the standard isobutyryl protection for G and benzoyl protection for A (*36*), or the more base-labile phenoxyacetyl protection for G and A, was used (*37*−*39*). Couplings with ∼13 μmol of amidite and ∼130 μmol of tetrazole for 12 min resulted in stepwise yields of 97−98%, determined by trityl monitoring at 498 nm. The crude products were cleaved from the support, base- and phosphate-deprotected with 3 mL of freshly saturated ethanolic ammonia (*32*). For RNA workup, all glass- and plasticware was autoclaved, nuclease-free sterile water was used, and buffers were autoclaved or sterile-filtered through 0.2 μm membranes.

G^{Pac}- and A^{Pac}-protected RNA was deprotected at 55 °C for 6 h, G^{Ibu}- and A^{Bz}- protected RNA for 16 h. The ammonia solution and washings of the support with EtOH/H_2O (60:40) were concentrated to dryness, and silyl groups were cleaved with 1.9 mL of predried (3 Å molecular sieve, 3 days) 1.1 M TBAF/THF solution with occasional vortexing. After quenching with 300 μL of 0.5 M ammonium acetate, partial evaporation of THF, and dilution to 2.5 mL with 50 mM ammonium acetate, the solution was desalted by elution through a 10 mL EconoPak DG 10 (BioRad) gel filtration column with 50 mM ammonium acetate. Oligonucleotide-containing 1 mL fractions were evaporated, dissolved in loading buffer, and purified by electrophoresis on denaturing 12% polyacrylamide gels (7 M urea, TBE buffer, 400 × 200 × 1.5 mm, 800 V, 9 A_{260} units of crude RNA per 2 cm slot). The main band was electroeluted in Schleicher & Schuell Elutraps (2 × 2 h, 200 V, TAE buffer), concentrated, ethanol-precipitated, and pelleted from 150 μL of 0.3 M sodium acetate. After washing with ethanol and drying, the pellets were dissolved in 200 μL of water and the RNA was renatured by heating for 4 min to 80 °C and cooling for 30 min to room temperature. Typically 200−450 μg of RNA was obtained from a 1 μmol synthesis.

Crude and purified samples of RNA (0.05−0.3 μg/μL), made from both sets of phosphoramidite monomers, were analyzed by capillary gel electrophoresis (*40*, *41*) in 100 μm i.d. Beckman eCAP U100P acrylamide-filled capillaries, 30 cm length, under denaturing conditions (7 M urea, 0.1 M Tris, 0.25 M sodium borate, pH 8.4) at 30° C with 370 V/cm and detection at 260 nm in a Beckman P/ACE instrument. As shown in Figure 1, gel-purified F8−RNA from both synthesis series was of homogeneous length. The purified 40-mer RNA was also analyzed by reversed-phase HPLC on a Rainin C4, 300 Å, 5 μm, 50 × 4.6 mm column and on a Hamilton polystyrene PRP-3, 300 Å, 10 μm, 125 × 4.1 mm column (data not shown), with 20 min gradients of 7−17% (Rainin) or 7−22% (Hamilton) acetonitrile in 0.1 M triethylammonium acetate, pH 7, at 1 mL/min and detection at 260 nm. About 0.1 A_{260} unit of the samples in

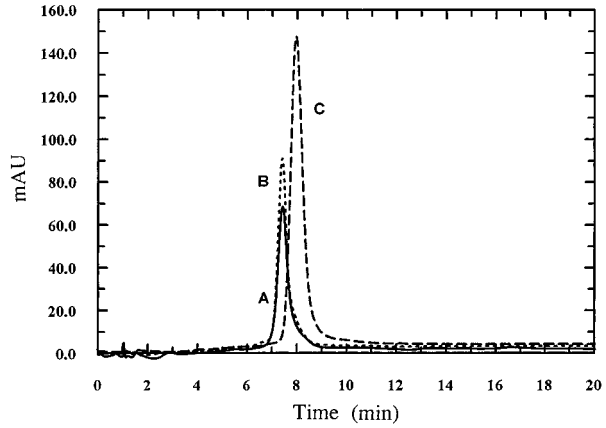

FIGURE 1: Analytical HPLC of purified (A) chemically synthesized 40-mer RRE (Milligen amidites), (B) chemically synthesized 40-mer RRE (Glen Res. amidites), and (C) transcribed 41-mer RRE, on a Hamilton PRP-3 column (300 Å, 10 μm, 150 × 4.1 mm) with detection at 260 nm.

10 μL of water was heated to 85 °C for 4 min and injected. The RNA from both phosphoramidite series exhibited single peaks on both types of columns (Figure 1).

The oligoribonucleotide was completely degraded by nuclease P1 in 30 mM sodium acetate, pH 5.3, 10 mM $ZnSO_4$, or by a mixture of ribonuclease A, T_1, and V_1 in 50 mM Tris (pH 7.6), 10 mM $MgCl_2$, 15 mM NaCl. Only peaks for the four ribonucleotide monophosphates were observed in capillary gel electrophoresis. Hypochromicity of the renatured 40-mer F8−RNA was 25%, determined by measuring the absorption at 260 nm before and after enzymatic degradation. For this measurement, 0.3 A_{260} unit was dissolved in 400 μL of 50 mM Tris (pH 7.6), 10 mM $MgCl_2$, 15 mM NaCl, renatured by heating to 80 °C and cooling to room temperature, and measured with buffer as reference. Two microliters of a mixture of RNases A (40 μg), T_1 (100 units), and V_1 (0.6 unit) in buffer was added to sample and reference in the cuvette and briefly stirred, and readings were taken until the end point of the reaction was reached.

For Rev binding assays, 5 pmol samples of F8−RNA were 5′-labeled with 25 μCi of [^{32}P]ATP and polynucleotide kinase (*42*). After gel filtration on a NAP-5 column (Pharmacia), phenol extraction, and ethanol precipitation, the labeled RNA was purified by electrophoresis on 12% polyacrylamide gels (7 M urea, 400 × 200 × 0.5 mm). After autoradiography, the isolated bands were electroeluted and ethanol-precipitated as described above and renatured in 50 μL of water by heating to 85 °C and slowly cooling to room temperature. High-affinity binding of the chemically synthesized F8−RNA 40-mers to Rev, with apparent K_d values of about 0.5 nM, was demonstrated by a filter binding assay with increasing amounts of Rev protein according to previously published procedures (*13*).

Enzymatic Synthesis of F8−RRE by T7 RNA Polymerase Transcription from Synthetic Double-Stranded DNA Templates. Enzymatic synthesis of RNA on the milligram scale by T7 RNA polymerase transcription from DNA templates was performed on the basis of published procedures (*43*, *44*). Oligodeoxyribonucleotides for double-stranded DNA templates, including the coding sequence for the 40-mer F8−RRE and a 17 bp upstream T7 promoter region, were chemically synthesized, gel-purified, and annealed in equimolar ratios to make 2 mM stock solutions.

Optimal transcription yields were achieved with a double-stranded template containing an additional G at the transcription start site, in combination with a highly concentrated T7 RNA polymerase preparation with about 300 units/mL (obtained from Dr. King Farrington). The coding strand had the sequence:

T7-Promoter 41-mer F8-RRE coding sequence

d(5' AAT T TA ATA CGA CTC ACT ATA **GGC ACT ATG GGC GCA GCG TCA ATG ACG CTG ACG GTA CAG GC** 3')

Large-scale transcription reactions were performed in 13.4 mL solutions containing 200 nM DNA template, 3 mM NTP's, 30 mM $MgCl_2$, 200 mM Tris (pH 8), 1.5 mM spermidine, 25 mM DTT, 250 mg/mL bovine serum albumin, and 67 μL of T7 RNA polymerase (about 300 units/mL) for 5 h at 37 °C. After addition of 0.8 mL of 0.5 M EDTA, heating to 80 °C for 10 min, and consecutive extractions with phenol/chloroform/isoamyl alcohol (24:1), chloroform/isoamyl alcohol, and diethyl ether, the aqueous solutions were desalted by gel filtration, concentrated, and purified by gel electrophoresis on four 12% polyacrylamide gels, 400 × 200 × 1.5 mm. RNA was recovered by electroelution, ethanol-precipitated from 0.3 M sodium acetate, and renatured in water. The yield was 110 A_{260} units, about 4.25 mg.

Analytical gel electrophoresis of transcribed 41-mer F8−RNA on a 12% polacrylamide gel, in comparison to chemically synthesized 40-mer F8−RNA, showed a homogeneous band for the 41-mer moving slightly slower than the 40-mer, without any indications of shorter fragments or $n+1$ or $n+2$ bands from nonspecific elongation. Analytical reversed-phase HPLC of a preheated sample of the transcribed 41-mer RNA on a Hamilton PRP-3 column (300 Å, 10 mm, 150 × 4.1 mm) showed a single peak with a slightly longer retention time than the chemically synthesized 40-mer F8−RRE (Figure 1).

The 41-mer RRE was completely degraded and dephosphorylated by treatment with nucleases A and T_1 and alkaline phosphatase in 50 mM Tris (pH 7.6), 10 mM $MgCl_2$, 3 mM NaN_3. Reversed-phase HPLC on a Nucleosil 100 5C18 column (250 × 4.6 mm) with isocratic elution with 0.1 M triethylammonium acetate, pH 7/acetonitrile (95:5) at 1 mL/min detected only the four monoribonucleosides in the correct ratio. Hypochromicity of the renatured 41-mer RNA, determined after enzymatic degradation, was 22.7%. The Rev saturation binding assay (*13*) with a ^{32}P-labeled aliquot showed high-affinity binding of the transcribed 41-mer RNA to Rev with a dissociation constant, determined at half-saturation, of about 0.5 nM.

Sample Preparation. Rev samples were diluted in Rev buffer [20 mM Tris (pH 7.5), 20 mM K_2SO_4, 50 mM $(NH_4)_2SO_4$, 1 mM DTT, 1 mM EDTA, 1.3 M NaCl or 0.1 M NaCl]. The typical Rev concentration used in the fluorescence experiments was 10 μM. RNAs were refolded by heating to 80 °C for 2 min and were allowed to cool slowly to room temperature and then on ice for about an hour. Aliquots of Rev were added to an RNA solution to form a 1:1 complex and incubated for at least 10 min prior to fluorescence measurements. Buffer solutions or buffer solutions containing RNA only were also measured under the same experimental conditions to correct for their contribution to the observed fluorescence.

The Rev deletion mutants M9Δ14 and M11Δ14 were dissolved in MES buffer (20 mM MES (pH 6.5), 3 mM NaN_3). Rev peptide samples were dissolved in the Rev buffer containing 0.1 M NaCl.

Time-Resolved Fluorescence Measurements. Fluorescence decay measurements were performed using the time-correlated single photon counting setup described in detail elsewhere (*45*). Samples were measured in quartz cuvettes (10 mm path length) and excited at 295 nm using the frequency-doubled output from a synchronously mode-locked and cavity-dumped rhodamine 6G dye laser (Coherent 702). Sample emission was collected at right angles to the excitation beam, collimated by a lens, passed through a motor-controlled polarizer, and focused on the entrance slit of a monochromator (JY H-10). The emission was monitored at 340 nm for Rev and at 350 nm for the peptides and Rev deletion mutants. A WG-335 filter (Schott) was used to block scattered laser light and solvent Raman emission. The filter was removed for measurements of decay-associated spectra. The output from the monochromator was detected by a microchannel plate photomultiplier (Hamamatsu R2809U-01). Time-resolved fluorescence decay profiles were acquired using standard time-correlated single photon counting electronics. Decays were recorded in 512 channels of an Ortec Norland 5510 multichannel analyzer using a sampling time of 36 ps per channel, or in 4096 channels of an Oxford PCA-3 multichannel analyzer with 9 ps per channel. For measurement of the isotropic fluorescence decay, the emission polarizer was oriented at 54.7° to the vertical excitation polarization. For fluorescence anisotropy decay measurements, the emission polarizer was alternated between vertical and horizontal directions every 30 s, and the decays collected with each polarizer setting were accumulated in separate memory segments of the multichannel analyzer. Movement of the polarizer and data accumulation in the multichannel analyzer were under computer control. All measurements were performed at 20 °C. Time-resolved emission data were transferred to either a Sun Sparc 4 or a Sparc LX workstation for analysis.

Data Analysis. Time-resolved fluorescence decay curves were fitted to a sum of discrete exponentials using nonlinear least-squares methods (*46*). The isotropic fluorescence decay was described by eq 1:

$$I(t) = g(t) \otimes K(t) \tag{1}$$

where $g(t)$ is the instrumental response function, which is convoluted (denoted by ⊗) with $K(t)$, the ideal fluorescence intensity. $K(t)$ was represented by eq 2:

$$K(t) = \sum_{i=1}^{N} \alpha_i \exp(-t/\tau_i) \tag{2}$$

where α_i and τ_i are the amplitude and lifetime for component i, respectively, and there are N components. The individual lifetimes and amplitudes were optimized for the best fit of eq 1 to the observed decay profile. The goodness of fit was judged by the reduced χ^2 value and by inspection of the weighted residuals from curve fitting.

The polarized fluorescence intensity decays were described by eqs 3 and 4:

$$I_{||}(t) = g(t)\otimes 1/3\{[1 + 2r(t)]K(t)\} \tag{3}$$

$$I_{\perp}(t) = g(t)\otimes 1/3\{[1 - r(t)]K(t)\} \tag{4}$$

where $I_{||}(t)$ and $I_{\perp}(t)$ are the time-resolved intensities of the parallel and perpendicular polarization components of the fluorescence, respectively. The time-dependent anisotropy, $r(t)$ was represented as in eq 5:

$$r(t) = \sum_{k=1}^{M} \beta_k \exp(-t/\phi_k) \tag{5}$$

Here, β_k and ϕ_k are the anisotropy amplitude and decay time for component k, respectively, and there are M anisotropy decay components. The anisotropy decay times and amplitudes were optimized for a simultaneous best fit of eqs 3−5 to $I_{||}(t)$ and $I_{\perp}(t)$, with the parameters appearing in $K(t)$ kept fixed at the values obtained from analysis of the isotropic fluorescence decay. The goodness of fit was judged as described above. The total anisotropy at time zero, r_0, was calculated by summing the β_k values (eq 6):

$$r_0 = \sum_{k=1}^{M} \beta_k \tag{6}$$

Decay-associated spectra (DAS) were obtained from a global fit of fluorescence decays collected at different emission wavelengths, with the common lifetimes linked across all data sets while optimizing the amplitudes for each decay (*47*). The DAS of each decay component was then calculated according to eq 7:

$$I_i(\lambda) = [\alpha_i(\lambda)\tau_i / \sum_{i=1}^{N} \alpha_i(\lambda)\tau_i] I_{ss}(\lambda) \tag{7}$$

where $\alpha_i(\lambda)$ is the amplitude for lifetime component i at emission wavelength λ, and $I_{ss}(\lambda)$ is the total steady-state fluorescence intensity at emission wavelength λ.

RESULTS

Time-Resolved Fluorescence of Rev. The results of the fluorescence lifetime analysis of Trp45 in Rev at 0.1 M NaCl are presented in Table 1. The isotropic fluorescence decay of Rev is well represented by a sum of four discrete lifetime components (reduced $\chi^2 = 1.0-1.2$). A typical decay profile is shown in Figure 2 along with the weighted residuals for a four-component fit. Decay-associated spectra (DAS) were determined for each decay component to further characterize the emission of Trp45. Fluorescence decays recorded at 5 nm intervals between 315 and 405 nm were globally analyzed with four linked lifetimes (global reduced $\chi^2 = 1.4$). The resulting DAS (Figure 3A), calculated according to eq 7, represent the contribution of each decay component to the overall steady-state emission spectrum of Rev. It is evident that the 1.8 ns decay component (τ_3) makes the greatest contribution to the steady-state emission of Trp45. The emission maximum at 345 nm indicates that this component reflects tryptophan in a relatively solvent-exposed environment. The DAS for the 0.57 ns (τ_2) and 4.6 ns (τ_4) decay components also exhibit emission maxima around 345 nm, but these components make smaller contributions to the

Table 1: Tryptophan Fluorescence Decay Parameters[a]

	lifetimes (ns)				amplitudes				
sample	τ_1 (±0.020)	τ_2 (±0.050)	τ_3 (±0.10)	τ_4 (±0.20)	α_1 (±0.02)	α_2 (±0.02)	α_3 (±0.02)	α_4 (±0.02)	$\langle\tau\rangle$ (ns)[b]
Rev[c]	0.115	0.572	1.82	4.63	0.21	0.28	0.40	0.11	1.42
M9Δ14[d]		0.496	1.93	4.64		0.21	0.47	0.32	2.50
M11Δ14[d]	0.121	0.630	1.95	4.74	0.13	0.33	0.41	0.14	1.69
Rev + F8−RRE[c]	0.092	0.540	1.66	3.93	0.16	0.36	0.39	0.09	1.21
Rev + 5S RNA[c]	0.081	0.465	1.57	4.05	0.27	0.33	0.33	0.07	0.98

[a] λ_{ex} = 295 nm, λ_{em} = 340 nm, 20 °C. Corrected for background. Intensity decays are fitted to a sum of four exponential components. The absence of an entry indicates that fewer than four lifetimes are resolved. [b] Mean fluorescence lifetime $\langle\tau\rangle = \sum\alpha_i\tau_i$. [c] Measured in Tris-HCl buffer (pH 7.5), 0.35 M NaCl. [d] Measured in MES buffer.

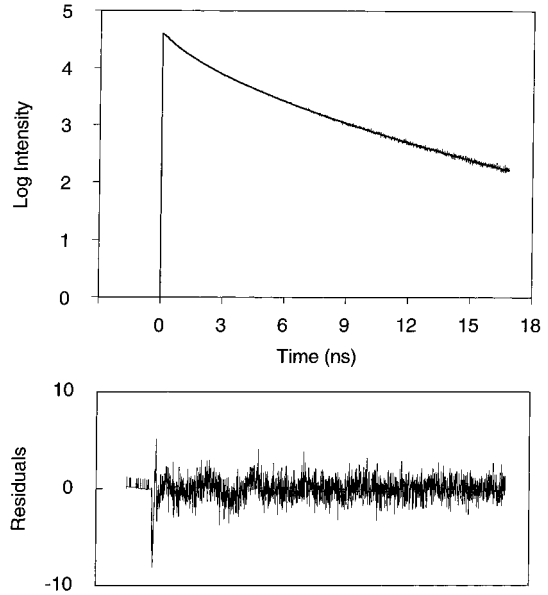

FIGURE 2: Isotropic fluorescence decay of Rev. The weighted residuals for a four-component fit are also shown. Rev concentration was 10 μM in Rev buffer (0.57 M NaCl). Excitation was at 295 nm, and the emission was observed at 340 nm.

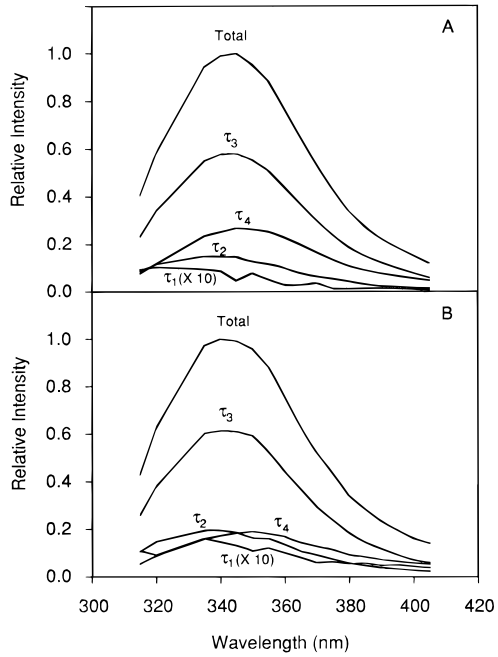

FIGURE 3: Decay-associated spectra (DAS) for Rev (A) and the Rev/F8−RRE complex (B). Rev concentration was 10 μM in Rev buffer (0.57 M NaCl). Excitation was at 295 nm. The RNA−protein mixture contained, in addition, 12 μM F8−RRE 40-mer.

overall emission. The DAS for the fastest decay component (τ_1) is significantly blue-shifted (emission maximum around 320 nm), suggesting that it represents tryptophan in a hydrophobic environment. This species makes the smallest contribution to the steady-state emission spectrum because of the very short lifetime (0.12 ns).

To check whether the short-lived, blue-shifted emission was due to a tyrosine residue of Rev, a peptide containing residues 8−26 of Rev was examined. This peptide contains a single tyrosine residue (corresponding to Tyr23 of Rev) but lacks tryptophan. The results confirmed that the tyrosine emission was negligible under the experimental conditions used to examine Rev (data not shown).

The fluorescence decay of Rev was measured at three different salt concentrations to ascertain whether any of the decay parameters depend on ionic strength. The results (not shown) indicate that the individual lifetimes and amplitudes do not vary significantly over the range of salt concentrations used (between 0.37 and 1.1 M NaCl).

The results of the fluorescence anisotropy decay analysis of Rev at 0.1 M NaCl are shown in Table 2. The anisotropy is well represented by two decay components (reduced χ^2 = 1.0−1.2). A typical fluorescence anisotropy decay for Rev is shown in Figure 4, together with the weighted residuals obtained from simultaneous fitting of the parallel

Table 2: Fluorescence Anisotropy Decay Parameters[a]

sample	ϕ_1 (ps)	ϕ_2 (ns)	β_1 (±0.005)	β_2 (±0.005)	r_0[b]
Rev[c]	679 ± 50	23 ± 3	0.032	0.228	0.260
Rev + F8−RRE[c]		30 ± 5		0.241	0.241
Rev + 5S RNA[c]		45 ± 8		0.261	0.261
P1[d]		0.082 ± 0.010		0.216	0.216
P2		0.472 ± 0.050		0.220	0.220
P3		0.432 ± 0.050		0.184	0.184
P4	34 ± 10	0.714 ± 0.050	0.073	0.166	0.239
P5	143 ± 10	1.10 ± 0.05	0.066	0.148	0.214
M9Δ14[e]	350 ± 50	11 ± 2	0.037	0.198	0.235
M11Δ14[e]	653 ± 50	23 ± 3	0.027	0.209	0.236

[a] Anisotropy decays are fitted to two components: $r(t) = \beta_1 e^{-t/\phi_1} + \beta_2 e^{-t/\phi_2}$. The absence of an entry indicates that the anisotropy decay is fitted with only one component. The temperature was 20 °C for all samples. [b] Total anisotropy at time zero. [c] Measured in Tris-HCl buffer (pH 7.5), 0.35 M NaCl. [d] All peptides measured in Tris-HCl buffer (pH 7.5), 0.1 M NaCl. [e] Measured in MES buffer.

and perpendicular polarization components of the intensity decays. The slow anisotropy decay component (23 ns) reports on overall tumbling of the protein, while the faster component (679 ps) reflects segmental motions of the protein or local rotation of Trp45. The flexibility evident in the rapid anisotropy decay component is consistent with a surface-

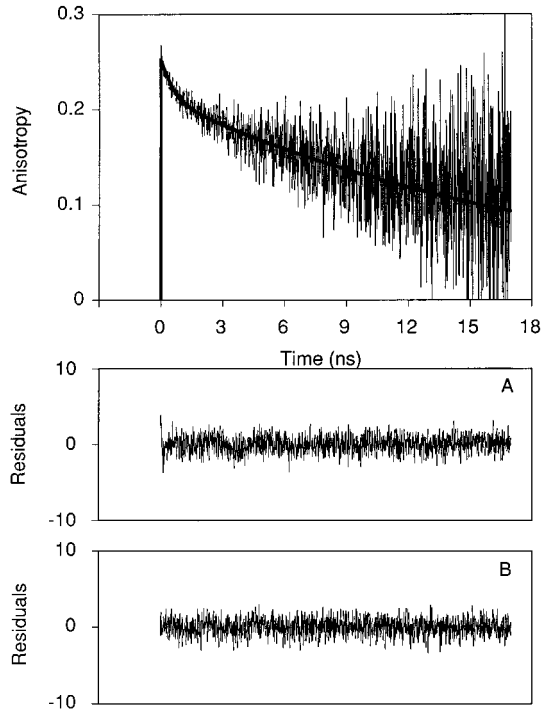

FIGURE 4: Anisotropy decay of Rev with the fitted curve for two decay components drawn as a solid line through the data. The weighted residuals from fitting the parallel component of the intensity decay are shown in (A), and those for the perpendicular component are shown in (B). Rev concentration was 10 μM in Rev buffer (0.57 M NaCl). Excitation was at 295 nm, and the emission was observed at 340 nm.

exposed environment for Trp45. The angular range of tryptophan motion was estimated from the anisotropy amplitudes using a model of diffusion within a cone (*48*). This yields a cone semi-angle of 17°, indicating that the local motion of Trp45 is relatively restricted. The rotational correlation time of Rev is independent of the salt concentration (between 0.37 and 1.1 M NaCl). However, the observed rotational correlation time of 23 ns is much larger than expected for a 12.9 kDa protein (corresponding to the molecular mass of Rev) with a spherical shape, which is calculated to be about 5.7 ns at 20 °C (*49*). This suggests the presence of Rev multimers under the experimental conditions.

Rev Peptides and C-Terminal Deletion Mutants. To further dissect the multicomponent intensity decay of Trp45 in Rev, small peptides and C-terminally deleted mutants of Rev were investigated. The fluorescence lifetimes of the Rev-related peptides (see Materials and Methods for peptide sequences) are presented in Table 3. In contrast to Rev, the fluorescence decays of the peptides are well represented by a sum of three discrete components (reduced $\chi^2 = 1.1-1.2$). In general, the three lifetimes for the peptides are similar to the three longest decay times observed for Rev (cf. Tables 1 and 3), indicating a common origin for these lifetime components in both the full-length protein and the various peptide fragments. The average fluorescence lifetimes for the peptides are longer than found for Rev, however, owing to the absence of the very fast decay component in the peptides. With the exception of P1, the individual lifetimes and amplitudes are similar for each peptide, although there appears to be a slight trend toward larger τ_3 values in the longer peptides (Table 3). The decay parameters for the

Table 3: Fluoresence Lifetime Analysis of Rev Peptides[a]

	lifetimes (ns)			amplitudes			
sample	τ_1 (±0.020)	τ_2 (±0.05)	τ_3 (±0.20)	α_1 (±0.02)	α_2 (±0.02)	α_3 (±0.02)	$\langle\tau\rangle$ (ns)[b]
P1	0.715	2.15	3.71	0.26	0.48	0.26	2.18
P2	0.442	1.99	4.19	0.22	0.44	0.33	2.36
P3	0.476	2.00	4.10	0.19	0.47	0.33	2.38
P4	0.585	2.14	4.35	0.20	0.47	0.33	2.56
P5	0.443	2.01	4.61	0.20	0.47	0.33	2.55

[a] $\lambda_{ex} = 295$ nm, $\lambda_{em} = 350$ nm, 20 °C. Measured in Tris-HCl buffer (pH 7.5), 0.1 M NaCl. Corrected for background. Intensity decays are fitted to a sum of three exponential components. [b] Mean fluorescence lifetime $\langle\tau\rangle = \sum\alpha_i\tau_i$.

dipeptide RW (P1) and the hexapeptide RRRRWR (P2) are noticably different, however, which probably reflects the influence of the C-terminal arginine residue flanking tryptophan in the hexapeptide. Taken together, these results suggest that the fluorescence decay properties of the tryptophan residue are influenced by one or both of the two flanking arginine residues, but are relatively insensitive to the more distant residues.

The fluorescence decay of the Rev deletion mutant M9Δ14 (lacking residues 68−112 at the C-terminus) is satisfactorily resolved into three lifetimes that are similar to those of the longer Rev peptides such as P5 (Table 1). The fluorescence decay of Rev M11Δ14 (residues 92−112 deleted), however, is resolved into four lifetimes (Table 1). The resulting lifetimes and amplitudes are typical of the full-length Rev protein.

The results of the fluorescence anisotropy decay measurements of the Rev peptides and C-terminal deletion mutants are summarized in Table 2. For the shorter peptides, the anisotropy decay is adequately represented by a single rotational correlation time. The rotational correlation time increases with the size of the peptide, reflecting a slower rate of overall tumbling. For the longer peptides, the addition of a fast component results in better fits to the anisotropy decay. This shorter correlation time (34−143 ps) presumably reflects segmental flexibility in the longer peptides. The anisotropy decays of the two Rev deletion mutants are also fitted to two components. The overall rotational correlation time (11 ns) is much longer for Rev M9Δ14 than for the largest peptide (P5), reflecting the larger size of Rev M9Δ14. The Rev M9Δ14 mutant has an additional 33 N-terminal residues and 16 more C-terminal residues than P5. The longest rotational correlation time is found for M11Δ14, 23 ns, about twice that of Rev M9Δ14, and identical with that of full-length Rev. The additional 22 amino acids present in Rev M11Δ14 compared with the M9Δ14 mutant cannot account for the change in rotational correlation time from 11 to 23 ns, which roughly corresponds to a doubling of the molecular volume of the particle. Therefore, a dimerization of the protein probably occurs.

Rev−RNA Complexes. The fluorescence decay of Trp45 was measured after binding Rev to the F8 fragment of the RRE. The F8 40-mer has been identified as a minimal binding element for high-affinity, specific Rev binding (*30*). The F8−RRE substrates were either chemically synthesized or transcribed from a complementary DNA template using T7 RNA polymerase (see Materials and Methods). The F8−RRE transcripts contained an extra G residue at the 5′-

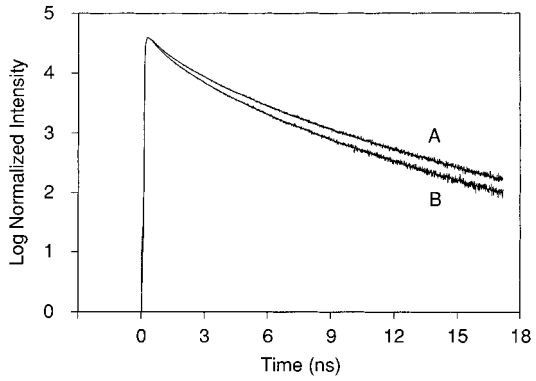

FIGURE 5: Isotropic fluorescence decays of Rev (A) and Rev/F8−RRE complex (B). Rev concentration was 10 μM in both cases in Rev buffer (0.57 M NaCl). The RNA−protein mixture contained, in addition, 12 μM F8−RRE 40-mer. Excitation was at 295 nm, and the emission was observed at 340 nm.

terminus, but this was not expected to influence the interaction with Rev. In fact, the transcribed F8 41-mer behaved identically to the chemically synthesized F8 40-mer in the spectroscopic experiments (data not shown). The effect of 5S RNA on the fluorescence decay of Rev was also examined to investigate the specificity of the Rev/F8−RRE interaction. In all cases, sufficient RNA was added to a sample of Rev (10 μM) to ensure that all the protein was bound. This was determined empirically by titrating Rev with the RNA of interest until there was no further change in the fluorescence decay profile. The measured decay was corrected for residual emission from the nucleic acids by subtracting the emission from a suitable blank sample measured under identical conditions.

Binding of the F8−RRE 40-mer to Rev results in a faster decay of tryptophan fluorescence (Figure 5). The fluorescence decay of bound Rev is well represented by four lifetimes (Table 1). The individual lifetimes for the Rev−RRE complex are shorter than the corresponding values for unbound Rev, especially τ_3 and τ_4 (Table 1). Similar results are obtained at two different salt concentrations (0.35 and 0.57 M NaCl). The DAS analysis of the Rev−RRE complex reveals a blue shift for the major decay component (τ_3) and a small redistribution of intensity among the minor lifetime components (Figure 3B). Complexation of Rev with 5S RNA produces very similar changes in the fluorescence lifetimes of Trp45 (Table 1).

The results of the fluorescence anisotropy decay measurements for Rev and its RNA complexes are summarized in Table 2. In contrast to free Rev, the anisotropy decays of the Rev−RNA complexes are well described by a single rotational correlation time. The rotational correlation time for overall tumbling increases from 23 ns to 30 ns upon binding of Rev to the F8−RRE 40-mer (Table 2), reflecting the increased size of the RNA−protein complex compared with the free protein. The rotational correlation time for the complex of Rev and 5S RNA is even larger (45 ns), which reflects the larger size of 5S RNA (130 nucleotides) compared with F8−RRE (40 nucleotides). It should be noted that the recovered rotational correlation times are much larger than the average fluorescence lifetime of Trp45 and consequently are subject to significant experimental uncertainty. The anisotropy decay results for the RNA−protein complexes should therefore be regarded as indicating trends in the overall sizes of the complexes rather than as giving precise estimates of the correlation times.

DISCUSSION

The single tryptophan residue of HIV-1 Rev, Trp45, has been used here as an intrinsic fluorescent probe of protein conformation and protein−RNA interactions. The tryptophan residue is located within the arginine-rich RNA-binding domain of Rev and is appropriately positioned, therefore, to report on the interaction of Rev with the RRE. To provide a framework for interpreting the time-resolved fluorescence properties of Trp45 in terms of protein structure, a series of Rev peptides spanning different regions of the arginine-rich domain and two C-terminal deletion mutants of Rev were also examined. In addition, the time-resolved fluorescence anisotropy decay of Trp45 has been used to probe the association state of Rev in solution and in protein/RNA mixtures.

The fluorescence decays of all the Rev peptides have been resolved into three separate components, represented by lifetimes of 0.45−0.72 ns, 2.0−2.2 ns, and 3.7−4.6 ns. In general, these lifetimes are only weakly dependent upon the length of the peptides, although there is a noticeable difference between the values for the dipeptide (RW) and the next largest peptide (RRRRWR). The multiple fluorescence lifetimes probably reflect three rotameric conformations of the tryptophan side chain that interconvert slowly on the fluorescence time scale, as suggested in a previous time-resolved fluorescence study of tryptophan dipeptides (*50*). The different fluorescence lifetimes of the tryptophan rotamers presumably arise from interactions of the indole ring with the main chain and one or both of the arginine residues flanking the tryptophan residue. However, judging by the relative insensitivity of the fluorescence decay kinetics to the overall length of the peptides, it appears that the more distant residues have little effect on the tryptophan fluorescence.

The same three fluorescence lifetimes are found for the Rev deletion mutant M9Δ14, which contains residues 1−67 of Rev. CD studies and theoretical modeling have shown that this region of Rev adopts a helix−loop−helix structure (*27*). Since the fluorescence decay parameters of this mutant are essentially identical with those of the longer peptides such as P5, it appears that none of the structural elements present within the helix−loop−helix motif, other than the nearest-neighbor arginine residues, have any significant effect upon Trp45. In contrast, inclusion of the Rev activation domain (residues 78−93) in the protein has a pronounced effect on the fluorescence decay kinetics of Trp45, as shown by the presence of four fluorescence lifetimes for RevM11Δ14 (containing residues 1−91 of Rev) or wild-type Rev. Three of these lifetimes (τ_2, τ_3, and τ_4; Table 1) are essentially identical with those observed for the peptides and exhibit spectral characteristics of a solvent-exposed tryptophan. These lifetimes presumably represent three rotameric conformations of the tryptophan side chain, with similar environments to those present in the larger peptide fragments. In contrast, the fourth lifetime is much shorter (τ_1, Table 1), and the DAS is significantly blue-shifted relative to the other components. Thus, the presence of the activation domain induces an additional tryptophan environment that is not present in the peptides or RevM9Δ14.

The unique tryptophan environment could be due to a direct interaction between the activation domain and Trp45, located in the RNA-binding domain. However, these two regions of Rev are functionally independent and are unlikely to be in direct contact. Alternatively, the activation domain may mediate the intermolecular association of two or more Rev molecules, which could also create a unique tryptophan environment. Consistent with this, the activation domain is required for multimerization of Rev on the RRE target sequence (*51*). Therefore, it is plausible that the short lifetime component observed for Trp45 represents a multimeric form of Rev, especially since Rev appears to be multimerized under the conditions of the fluorescence experiments (see below). The blue-shifted emission of this species could be due to a nonpolar environment surrounding the indole ring. In addition, specific interactions of the indole ring with charged groups can also cause a blue-shift in emission, although the blue-shifted DAS observed for Trp45 is likely dominated by the more common hydrophobic interaction. Thus, Trp45 may become buried during the higher order assembly of Rev, suggesting that it contributes directly to the oligomerization process. This is consistent with evidence from mutational studies indicating that replacement of Trp45 by glycine abolishes oligomerization of Rev (*52*). Finally, although only a single fluorescence lifetime was resolved, the present results do not necessarily prove that the buried tryptophan exhibits monoexponential fluorescence decay. For example, the buried tryptophan may exhibit additional lifetime components that are indistinguishable from τ_2, τ_3, and τ_4.

The fluorescence anisotropy decay data provide more direct information on the self-association of Rev. Both wild-type Rev and Rev M11Δ14 appear to be multimerized under the conditions of the experiments, as shown by a rotational correlation time of 23 ns, which is much larger than expected for a Rev monomer (5.7 ns for spherical geometry). A number of previous studies have shown that Rev can self-associate, either in solution or in the presence of the RRE target sequence (*17*, *22*, *25*, *26*, *52*−*54*). Two earlier reports suggested that Rev exists as a stable tetramer in solution (*25*, *52*). Interestingly, the rotational correlation time of Rev is about 4 times larger than expected for a spherical monomer, which is suggestive of a tetramer. However, the agreement is probably fortuitous because Rev is likely to be elongated rather than spherical. Consistent with this, the M9Δ14 deletion mutant also rotates more slowly than expected (rotational correlation time of 11 ns, Table 2), even though this mutant is known to be defective in multimerization and is not expected to undergo significant higher order assembly (*51*). The discrepancy between the observed rotational correlation time and the theoretical value for a monomer suggests that the M9Δ14 mutant has a markedly asymmetric and elongated overall shape, consistent with the predicted helix−loop−helix structure for this region of Rev (*27*). Asuming that the rotational correlation time of 11 ns corresponds to a monomeric species of Rev, the observed rotational correlation time of 23 ns for wild-type Rev suggests that the predominant oligomeric species is a dimer under the conditions of the fluorescence experiments. The Rev dimer is also likely to be asymmetric, accounting for the anomalously slow rotation time.

Taken together, the fluorescence lifetime and anisotropy decay data indicate that Rev is primarily a dimer (with each monomer containing three tryptophan rotamers, represented by the fluorescence lifetimes τ_2, τ_3, and τ_4) with a population of higher order oligomers (represented by τ_1). This is consistent with a study by Cole et al. (*22*) showing that Rev can actually polymerize in solution to form a variety of oligomeric species, depending on the protein concentration. This oligomerization of Rev is known to occur at concentrations below the ones used in our experiments and is practically independent of monovalent salt concentration from 0.15 to 2 M (*22*). The anisotropy decay data presented here also indicate that the rotational correlation time of Rev, and thus the distribution of Rev oligomers, is independent of salt concentration (from 0.37 to 1.1 M). Moreover, the anisotropy decay and fluorescence lifetime data indicate that significant oligomerization of Rev only occurs in the presence of the activation domain. Previous studies have emphasized the importance of the N-terminal region of Rev in mediating oligomerization (*52*, *53*). The present results suggest that the activation domain also contributes to self-association of Rev.

The binding of Rev to F8−RRE is reflected in the time-resolved fluorescence of Trp45. The decay of the fluorescence intensity is more rapid than observed for free Rev (Figure 5), indicating that Trp45 is partially quenched within the RNA−protein complex, and there is a blue shift in the emission, indicating that the tryptophan residue is in a more hydrophobic environment than in the free protein (Figure 3B). Moreover, whereas free Rev exhibits both fast and slow anisotropy decay components, reflecting local rotation of Trp45 and overall protein tumbling, respectively, only the latter is observed for the protein−RNA complex, indicating that the local rotation is blocked. Taken together, these observations indicate that Trp45 directly interacts with the RNA structure. This conclusion is consistent with a recent NMR-based structural study of a model Rev peptide bound to the internal loop region of the RRE, which shows that Trp45 makes a hydrophobic contact with a bulged adenine base (*29*). The present results showing an interaction between Trp45 of Rev and the RRE suggest that the mode of binding of the peptide is similar to that of the full-length protein, at least insofar as the tryptophan residue is concerned. The existence of a contact between Trp45 and the RRE is also consistent with mutational data showing that replacement of Trp45 by arginine or glycine strongly reduces binding of Rev to the RRE (*52*).

The anisotropy decay data indicate that the rotational correlation time of Rev increases from 23 ns to 30 ns upon binding to F8−RRE. An earlier study has reported that the F8 fragment of the RRE only binds a single Rev molecule (*30*), whereas Rev appears to exist primarily as a dimer under the conditions of the fluorescence anisotropy experiments. This suggests that the Rev dimers must dissociate in order to bind to the small F8−RRE molecule. To investigate this possibility, we sought to calculate the rotational correlation time expected for a 1:1 complex of Rev and F8−RRE. However, it is difficult to calculate the rotational correlation time for a 1:1 complex because the three-dimensional structure is unknown. It is possible, however, to estimate the rotational correlation time of the F8−RRE fragment itself, recognizing that this provides only a lower limit for the

complex, because the structure of a similar RRE fragment bound to a Rev peptide has been solved by NMR methods, as noted above (*29*). The 34 nucleotide RRE fragment in the NMR structure contains most of the F8 fragment, including the internal loop region and the flanking helixes. The purine-rich internal loop significantly widens the overall diameter of the molecule, which can be approximated by a cylinder with dimensions of 64 Å (length) and 29 Å (diameter). The rotational diffusion constants for this cylinder were calculated using the theory of Tirado and Garcia de la Torre (*55*). Three unique correlation times are expected for a cylindrical shape, which in the present case assume values of 9.2, 17.8, and 25.8 ns. Experimentally, it is difficult to resolve three correlation times, and one expects to observe an effective average value, between 9 ns and 26 ns, depending on the orientation of the emission dipole. Given that a Rev monomer is also elongated and has a rotational correlation time around 11 ns, and that the F8 40-mer is slightly larger than the RRE fragment used in the hydrodynamic calculations, it is expected that the rotational correlation time of a 1:1 complex of Rev and F8−RRE will fall in the 20−35 ns range. While these calculations are not conclusive, they suggest that the observed correlation time of 30 ns is reasonable for a 1:1 complex of Rev and F8−RRE.

Despite the difference in the overall association state of Rev, it appears that the same substates of tryptophan are present in the free and bound forms of Rev. Thus, the decay profile for the Rev/F8−RRE complex has been resolved into four discrete components that correlate with those observed for the free protein. In the case of the three longest decay components (τ_2, τ_3, and τ_4), this implies that the side chain of Trp45 can still populate three rotameric conformations, even when Rev is bound to the F8−RRE. However, free rotation of the Trp side chain is blocked in the complex, as noted above. The occurrence of the fast decay component (τ_1) implies that higher order Rev oligomers are also present in the protein−RNA mixtures. However, the present data do not prove that this minor species is actually bound to the RRE. It is possible that the oligomeric species represented by τ_1 is too large to bind to the small F8 molecule, does not undergo significant dissociation, and simply remains free in solution.

Characteristic changes in the fluorescence lifetime and anisotropy decay of Trp45 are also observed upon addition of 5S RNA to Rev. The binding is clearly shown by the increase of the rotational correlation time of Rev, which is greater for 5S RNA than for F8−RRE owing to the larger size of the RNA (Table 2). Judging by the similarity of the fluorescence decay parameters, the environment of Trp45 is essentially identical, regardless of whether Rev is bound to 5S RNA or to F8−RRE. 5S RNA is frequently used in competition analyses of protein−RNA interactions, because it is reasonably small and readily available. In fact, 5S RNA turned out to be the best "nonspecific" competitor for Rev−RRE complexes tried so far in our laboratory (data not shown). Knowing that Rev is basically a "guanosine-binding" protein, this effectiveness in competitive binding was attributed to the relatively high guanine nucleotide content (41 of 120 nucleotides = 34.6% are G). More recently it was reported that transcription factor IIIA (TFIIIA) contains a sequence element with homology to the activation domain of HIV-1 Rev which can efficiently substitute for this domain in inducing the nuclear export of late HIV-1 mRNAs (*56*). Given the similar changes observed in the fluorescence decay behavior, it appears that Trp45 of Rev may interact with 5S RNA and F8−RRE in a similar manner. For example, Trp45 may interact with an extrahelical base in 5S RNA, similar to the interaction between Trp45 and the bulged adenine base of the RRE (*29*). Therefore, it appears that in addition to having functionally equivalent nuclear export signal elements, Rev and TFIIIA can also bind to the same target RNAs, suggesting that these two proteins access similar or identical RNA-export pathways.

CONCLUSIONS

The environment of the lone tryptophan residue in HIV-1 Rev, Trp45, located in the RNA-binding domain of the protein, has been characterized by means of time-resolved fluorescence spectroscopy. The fluorescence decay kinetics of this single tryptophan residue are surprisingly complex, revealing the presence of four distinguishable species on the time scale of the fluorescence emission. This complexity stems from significant conformational heterogeneity, at the level of both the local orientation of the tryptophan side chain (rotamers) and the overall oligomeric state of the protein (dimers and higher order oligomers). The anisotropy decay data for the C-terminal deletion mutants indicate that the activation domain is required for self-association of Rev. Trp45 appears to directly interact with the RRE, resulting in a shortening of the average fluorescence lifetime and a restriction of the internal motion of the tryptophan side chain. The anisotropy decay data are consistent with the formation of a 1:1 complex between Rev and F8−RRE, suggesting that Rev dimers present in solution dissociate upon binding to this small RRE fragment. The fluorescence lifetime changes are similar for F8−RRE and 5S RNA, providing structural evidence for comparable RNA export pathways in eucaryotic HIV-1 infected and noninfected cells. This study also highlights the ability of the time-resolved fluorescence techniques to provide novel structural information on large, flexible, and multimeric proteins, such as Rev, that are difficult to study by X-ray crystallographic or NMR methods.

REFERENCES

1. Emerman, M., Vazeux, R., and Peden, K. (1989) *Cell 57*, 1155−1165.
2. Lu, X., Heimer, J., Rekosh, D., and Hammarskjold, M.-L. (1990) *Proc. Natl. Acad. Sci. U.S.A. 87*, 7598−7602.
3. Malim, M. H., Hauber, J., Fenrick, R., and Cullen B. R. (1989) *Nature 338*, 254−257.
4. Chang, D. D., and Sharp, P. A. (1989) *Cell 59*, 789−795.
5. Sodroski, J., Goh, W. C., Rosen, C., Dayton, A., Terwilliger, E., and Haseltine, W. (1986) *Nature 321*, 412−417.
6. Feinberg, M. B., Jarrett, R. F., Aldovini, A., Gallo, R. C., and Wong-Staal, F. (1986) *Cell 46*, 807−817.
7. Rosen, C. A., Terwilliger, E., Dayton, A., Sodroski, J. G., and Haseltine, W. A. (1988) *Proc. Natl. Acad. Sci. U.S.A. 85*, 2071−2075.
8. Dayton, E. T., Powell, D. M., and Dayton, A. I. (1989) *Science 246*, 1625−1629.
9. Hadzopoulou-Cladaras, M., Felber, B. K., Cladaras, C., Athanassopoulos, A., Tse, A., and Pavlakis, G. N. (1989) *J. Virol. 63*, 1265−1274.

10. Heaphy, S., Finch, J. T., Gait, M. J., Karn, J., and Singh, M. (1991) *Proc. Natl. Acad. Sci. U.S.A. 88*, 7366−7370.
11. Bartel, D. P., Zapp, M. L., Green, M. L., and Szostak, J. W. (1991) *Cell 67*, 529−536.
12. Tiley, L. S., Malim, M. H., Tewary, H. K., Stockley, P. G., and Cullen, B. R. (1992) *Proc. Natl. Acad. Sci. U.S.A. 89*, 758−762.
13. Daly, T. J., Cook, K. S., Gray, G. S., Maione, T. E., and Rusche, J. R. (1989) *Nature 342*, 816−819.
14. Zapp, M. L., and Green, M. R. (1989) *Nature 342*, 714−716.
15. Cochrane, A. W., Chen, C.-H., and Rosen, C. A. (1990) *Proc. Natl. Acad. Sci. U.S.A. 87*, 1198−1202.
16. Malim, M. H., Tiley, L. S., Mc Carn, D. F., Rusche, J. R., Hauber, J., and Cullen, B. R. (1990) *Cell 60*, 675−683.
17. Olsen, H. S., Nelbock, P., Cochrane, A. W., and Rosen, C. A. (1990) *Science 247*, 845−848.
18. Kjems, J., Calnan, B. J., Frankel, A. D., and Sharp, P. A. (1992) *EMBO J. 11*, 1119−1129.
19. Malim, M. H., Bohnlein, S., Hauber, J., and Cullen, B. R. (1989) *Cell 58*, 205−214.
20. Mermer, B., Felber, B. K., Campbell, M., and Pavlakis, G. N. (1990) *Nucleic. Acids Res. 18*, 2037−2044.
21. Venkatesh, L. K., and Chinnadurai, G. (1990) *Virology 178*, 327−330.
22. Cole, J. L., Gehman, J. D., Shafer, J. A., and Kuo, L. C. (1993) *Biochemistry 32*, 11769−11775.
23. Mann, D. A., Mikaélian, I., Zemmel, R. W., Green, S. M., Lowe, A. D., Kimura, T., Singh, M., Butler, P. J. G., Gait, M. J., and Karn, J. (1994) *J. Mol. Biol. 241*, 193−207.
24. Zemmel, R. W., Kelley, A. C., Karn, J., and Butler, P. J. G. (1996) *J. Mol. Biol. 258*, 763−777.
25. Nalin, C. M., Purcell, R. D., Antelman, D., Mueller, D., Tomchak, L., Wegrzynski, B., McCarney, E., Toome, V., Kramer, R., and Hsu, M.−C. (1990) *Proc. Natl. Acad. Sci U.S.A. 87*, 7593−7597.
26. Wingfield, P. T., Stahl, S. J., Payton, M. A., Venkatesan, S., Misra, M., and Steven, A. C. (1991) *Biochemistry 30*, 7527−7534.
27. Auer, M., Gremlich, H.-U., Seifert, J.-M., Daly, T. J., Parslow, T. G., Casari, G., and Gstach, H. (1994) *Biochemistry 33*, 2988−2996.
28. Scanlon, M. J., Fairlie, D. P., Craik, D. J., Englebretsen, D. R., and West, M. L. (1995) *Biochemistry 34*, 8242−8249.
29. Battiste, J. L., Mao, H., Rao, S., Tan, R., Muhandiram, D. R., Kay, L. E., Frankel, A. D., and Williamson, J. R. (1996) *Science 273*, 1547−1551.
30. Cook, K. S., Fisk, G. J., Hauber, J., Usman, N., Daly, T. J., and Rusche, J. R. (1991) *Nucleic Acids Res. 19*, 1577−1583.
31. Daly, T. J., Doten, R. C., Rennert, P., Auer, M., Jaksche, H., Donner, A., Fisk, G., and Rusche, J. R. (1993) *Biochemistry 32*, 10497−10505.
32. Scaringe, S. A., Francklyn, C., and Usman, N. (1990) *Nucleic Acids Res. 18*, 5433−5441.
33. Wu, T., Ogilvie, K. K., and Pon, R. T. (1988) *Tetrahedron Lett. 29*, 4249−4252.
34. Ogilvie, K. K., Usman, N., Nicoghosian, K., and Cedergren, R. J. (1988) *Proc. Natl. Acad. Sci. U.S.A. 85*, 5764−5768.
35. Usman, N., Ogilvie, K. K., Jiang, M.-Y., and Cedergren, R. J. (1987) *J. Am. Chem. Soc. 109*, 7845−7854.
36. Schaller, H., Weimann, G., Lerch, B., and Khorana, H. G. (1963) *J. Am. Chem. Soc. 85*, 3821.
37. Chaix, C., Duplaa, A. M., Gasparutto, D., Molko, D., and Teoule, R. (1989) *Nucleic Acids Res. Symp. Ser. 21*, 45−46.
38. Chaix, C., Molko, D., and Teoule, R. (1989) *Tetrahedron Lett. 30*, 71−74.
39. Wu, T., Ogilvie, K. K., and Pon, R. T. (1989) *Nucleic Acids Res. 17*, 3501−3517.
40. Cohen, A. S., Najarian, D. R., Paulus, A., Guttman, A., Smith, J. A., and Karger, B. L. (1988) *Proc. Natl. Acad. Sci. U.S.A. 85*, 9660−9663.
41. Guttman, A., Nelson, R. J., and Cooke, N. (1992) *J. Chromatogr. 593*, 297−303.
42. Cobianchi, F., and Wilson, S. H. (1987) *Methods Enzymol. 152*, 94−112.
43. Milligan, J. F., Groebe, D. R., Witherall, G. W., and Uhlenbeck, O. C. (1987) *Nucleic Acids Res. 15*, 8783−8798.
44. Wyatt, J. R., Chastain, M., and Puglisi, J. D. (1991) *BioTechniques 11*, 764−769.
45. Guest, C. R., Hochstrasser, R. A., Sowers, L. C., and Millar, D. P. (1991) *Biochemistry 30*, 3271−3279.
46. Bevington, P. R. (1969) *Data Reduction and Error Analysis for the Physical Sciences*, McGraw-Hill, New York.
47. Knuston, J. R., Walbridge, D. G., and Brand, L. (1982) *Biochemistry 21*, 4671−4679.
48. Kinosita, K., Kawato, S., and Ikegami, A. (1977) *Biophys. J. 20*, 289−305.
49. Cantor, C. R., and Schimmel, P. R. (1980) *Biophysical Chemistry. Part II: Techniques for the Study of Biological Structure and Function* W. H. Freeman & Co., New York.
50. Chen, R. F., Knutson, J. R., Ziffer, H., and Porter, D. (1991) *Biochemistry 30*, 5184−5195.
51. Daly, T. J., Rennert, P., Lynch, P., Barry, J. K., Dundas, M., Rusche, J. R., Doten, R. C., Auer, M., and Farrington, G. K. (1993) *Biochemistry 32*, 8945−8954.
52. Zapp, M. L., Hope, T. J., Parslow, T. G., and Green, M. R. (1991) *Proc. Natl. Acad. Sci. U.S.A. 88*, 7734−7738.
53. Malim, M. H., and Cullen, B. R. (1990) *Cell 65*, 241−248.
54. Daly, T. J., Cook, K. S., Fisk, G., Jensen, D., Hauber, J., Jaschke, H., and Rusche, J. R. (1991) in *Genetic Structure and Regulation of HIV* (Haseltine, W. A., and Wong-Staal, F., Eds.) pp 135−142, Raven, New York.
55. Tirado, M. M., and Garcia de la Torre, J. (1980) *J. Chem. Phys. 73*, 1986−1993.
56. Fridell, R. A., Fischer, U., Lührmann, R., Meyer, B. E., Meinkoth, J. L., Malim, M. H., and Cullen, B. R. (1996) *Proc. Natl. Acad. Sci. U.S.A. 93*, 2936−2940.

BI9719096